Bioorganic & Medicinal Chemistry 18 (2010) 2394–2401

Contents lists available at ScienceDirect

Bioorganic & Medicinal Chemistry

journal homepage: www.elsevier.com/locate/bmc

^{18}F Labeled benzimidazole derivatives as potential radiotracer for positron emission tomography (PET) tumor imaging

Shuting Zhang [a], Xiao Wang [a,*], Yong He [a], Rui Ding [a], Hang Liu [a], Jingli Xu [a], Man Feng [a], Guixia Li [a], Ming Wang [a], Cheng Peng [b], Chuanmin Qi [a,*]

[a] Key laboratory of Radiopharmaceuticals, College of Chemistry, Beijing Normal University, Beijing 100875, People's Republic of China
[b] Center of PET, Xuan Wu Hospital, Beijing 100053, People's Republic of China

ARTICLE INFO

Article history:
Received 28 December 2009
Revised 25 February 2010
Accepted 26 February 2010
Available online 6 March 2010

Keywords:
^{18}F
Benzimidazole derivatives
Bendamustine
Positron emission tomography

ABSTRACT

This article reported the synthesis and bioevaluation of two [^{18}F] labeled benzimidazole derivatives, 4-(5-(2-[^{18}F] fluoro-4-nitrobenzamido)-1-methyl-1*H*-benzimidazol-2-yl) butanoic acid ([^{18}F] FNBMBBA, [^{18}F]a1) and 3-(2-fluoroethyl)-7-methyl-2-propyl-3*H*-benzimidazole-5-carboxylic acid ([^{18}F] FEMPBBA, [^{18}F]b1) for PET tumor imaging. The preparation [^{18}F] FEMPBBA was completed in 1 h with overall radiochemical yield of 50–60% (without decay corrected). Biodistribution assay in S180 tumor bearing mice of both compounds were carried out, and the results are both meaningful. [^{18}F] FEMPBBA which can be taken as a revision of [^{18}F] FNBMBBA got an excellent result, and has significant advantages in some aspects compared with L-[^{18}F] FET and [^{18}F]-FDG in the same animal model, especially in tumor/brain uptake ratio. The tumor/brain uptake ratio of [^{18}F] FEMPBBA gets to 4.81, 7.15, and 9.8 at 30 min, 60 min and 120 min, and is much higher than that of L-[^{18}F] FET (2.54, 2.92 and 2.95) and [^{18}F]-FDG (0.61, 1.02, 1.33) at the same time point. The tumor/muscle and tumor/blood uptake ratio of [^{18}F] FEMPBBA is also higher than that of L-[^{18}F] FET at 30 min and 60 min. This result indicates compound [^{18}F] FEMPBBA is a promising radiotracer for PET tumor imaging.

1. Introduction

Benzimidazole and its derivatives are a kind of compound which exerts a wide range of biological activities, such as anti-inflammatory,[1–3] histamine-H3 antagonist,[4,5] anticancer[6,7] and antimetabolite.[8] For their varied biological activities, benzimidazole derivatives have attracted continuing interest over the years and were widely applied as an important pharmacophore or building block in drug discovery.[9–11] Bendamustine is such a representative drug which contains the structure of benzimidazole and is widely used as an antitumor agent in clinical.

Bendamustine is a DNA-alkylating agent shown clinical activity against various human cancers including non-Hodgkin's lymphoma,[12,13] chronic lymphocytic leukemia,[14,15] breast cancer[16,17] and small-cell lung cancer.[18,19] It contains three parts in its structure: a 2-chloroethylamine alkylating group, a benzimidazole ring, and a butyric acid side chain. After the study of the action mechanism and clinical activity of bedamustine, investigators found it displays a distinct pattern of activity unrelated to other nitrogen mustard DNA-alkylating agents such as cyclophosphamide, chlorambucil and melphalan, which have the same alkylating group. Moreover, there was no conclusion about the role of 4-(1-methyl-1*H*-benzimidazol-2-yl) butanoic acid group plays in making bendamustine behavior so unique.[20,21]

Our group has been trying to develop some novel ^{18}F labeled radiotracers for positron emission tomography (PET) imaging especially for tumor imaging. PET is widely applied in clinical for tumor imaging nowadays.[22] Of all the most commonly used positron isotopes employed in PET, ^{18}F is most favorable due to its optimal physical half-life ($t_{1/2}$ = 110 min).[23] It is well established that [^{18}F]-FDG is the most successful and widely used commercial PET radiopharmaceutical in the clinical.[24] However as there are also defects of [^{18}F]-FDG,[25–28] some other radiotracers were developed by labeling bioactive compounds with ^{18}F such as [^{18}F]-FET[29] and [^{18}F]-FLT[30,31] as alternate radiotracers. As benzimidazole derivatives also have a wide range of bioactivity and the structure is special compared with the existed radiotracers, we are really interested about whether the ^{18}F labeled benzimidazole derivatives can get a good result at PET tumor imaging.

However, the labeling and application of compounds containing benzimidazole nucleus in PET imaging were rarely reported. Therefore, we decided to label benzimidazole derivatives based on the structure of the building block of bendamustine with ^{18}F, not only because bendamustine is a representative drug which contains the structure of benzimidazle, but also because it is the building block of bendamustine which made this drug a unique DNA-alkylating agent.

* Corresponding author. Tel.: +86 136 8138 0097; fax: +86 010 588 02075.
E-mail address: qicmin@sohu.com (C. Qi).

0968-0896/$ - see front matter © 2010 Elsevier Ltd. All rights reserved.
doi:10.1016/j.bmc.2010.02.060

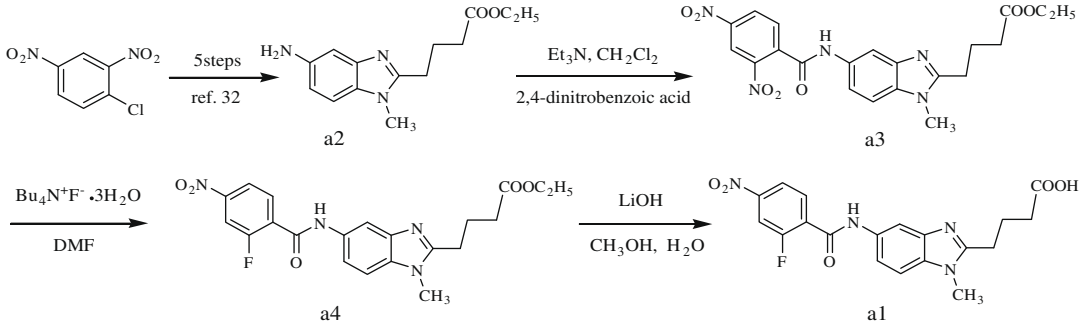

Scheme 1.

For this purpose we designed and synthesized [^{18}F] 4-(5-(2-fluoro-4-nitrobenzamido)-1-methyl-1*H*-benzimidazol-2-yl)butanoic acid ([^{18}F] FNBMBBA). It is the labeling of 4-(1-methyl-1*H*-benzimidazol-2-yl) butanoic acid (BBA, building block of bendamustine) by the introducing of 2,4-dinitrobenzoyl group at 5- of benzimidazole ring (Scheme 1). After that, we designed and synthesized (Scheme 2) another compound [^{18}F] 3-(2-fluoroethyl)-7-methyl-2-propyl-3*H*-benzimidazole-5-carboxylic acid ([^{18}F] FEMPBBA). It can be taken as a revision of the structure of [^{18}F] FNBMBBA, the carboxylic group was switched to a benzoic acid at the ring of benzimidazole, and it was labeled by introducing an ethyltosylate group at 3- of benzimidazole ring. A series of experiment was carried out in order to evaluate the bioactivity of both compounds.

2. Results and discussion

2.1. Radiochemistry

Both the radiosynthesis of compound [^{18}F] FEMPBBA and [^{18}F] FNBMBBA was carried out by the nucleophilic substitution of $^{18}F^{-}$ using [^{18}F] $K_{2.2.2}$/KF complex by the following procedure (Scheme 3).

[^{18}F] FNBMBBA was synthesized in approximately 100 min with high radiochemical yields (35–45% without decay corrected), and the radiochemical purity above 99%. The retention time of [^{18}F] FNBMBBA was 6.4 min (Altech C18 column 250 × 4 mm, CH_3CN/H_2O = 30:70 [vol/vol], 3 mL/min).

For the preparation [^{18}F] FEMPBBA, the purification was used by Sep-Pak Silica Plus cartridge instead of preparative HPLC method, which resulted in a shorter time of about only 1 h with overall radiochemical yield of 50–60% (without decay corrected), and the radiochemical purity was above 99%. The retention time of [^{18}F] FEMPBBA was 6.8 min (Altech C18 column 250 × 4 mm, CH_3CN/H_2O = 30:70 [vol/vol], 1 mL/min). The HPLC chromatograms of both compounds were shown in Figure 1.

2.2. Stability of [^{18}F] FNBMBBA and [^{18}F] FEMPBBA in plasma

As the results of HPLC analysis for both compounds indicate, they are all stable in the plasma after incubation for 3 h.

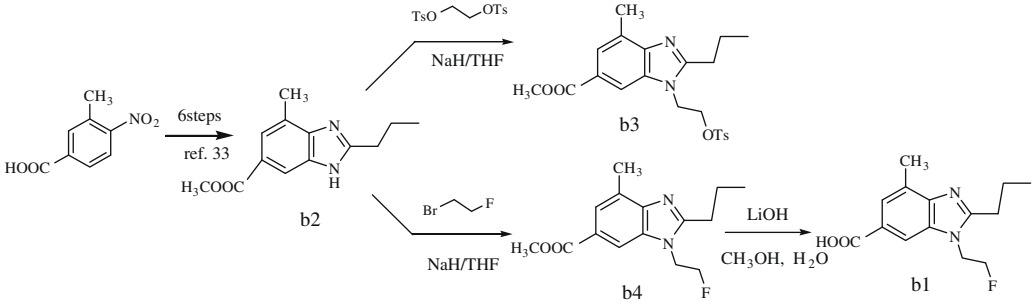

Scheme 2.

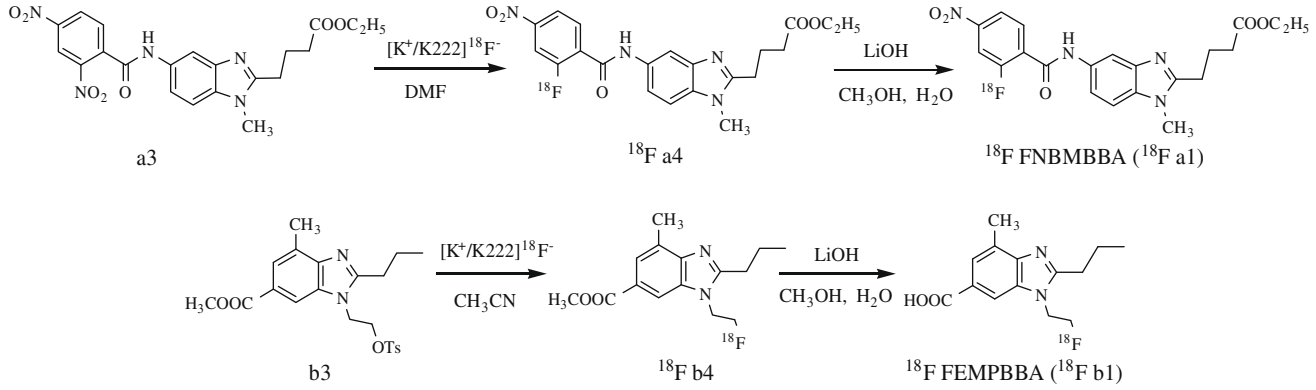

Scheme 3. Radiosynthesis procedures of [^{18}F] FEMPBBA and [^{18}F] FNBMBBA.

2.3. Measurement of partition coefficient

The partition coefficient of compound [^{18}F] FNBMBBA and [^{18}F] FEMPBBA was determined to be log P = −1.79 and −0.50. It suggests that the lipophilicity of compound [^{18}F] FEMPBBA is much higher than that of [^{18}F] FNBMBBA.

2.4. Biodistribution of [^{18}F] FNBMBBA and[^{18}F] FEMPBBA in S180 bearing mice

As the biodistribution result of [^{18}F] FNBMBBA shown in Table 1, the accumulation of this compound in all of the organs or tissue was highest in the 5 min post injection and then decreased. After that the activity in all organs or tissue decreased rapidly and this compound was quickly excreted out from the body through kidney after 60 min, and there is nearly no accumulation in the brain of this compound. We conclude this quickly clearance rate of [^{18}F] FNBMBBA is due to its high hydrophilicity.

Although the uptake in tumor of [^{18}F] FNBMBBA is comparably low, the clearance rate in the tumor is slower than in other organs or tissue, as time lapses, the activity in the tumor exceeds than that in most other organs or tissue. Consequently, [^{18}F] FNBMBBA has a high tumor/muscle uptake ratio which gets to 2.08 and 1.71 at 15 min and 60 min.

For [^{18}F] FEMPBBA (Table 2), the initial uptake in the tumor was 2.28 ± 0.27%ID/g at 5 min, although it decreased as the time lapsed, the rate of decrease was much slower than in other organs. That makes the activity of [^{18}F] FEMPBBA in the tumor remain at a certain level in a long period with only a little decrease: 1.49 ± 0.13%ID/g at 15 min, 1.41 ± 0.26%ID/g at 30 min and 1.36 ± 0.42%ID/g at 60 min. On the other hand, the activity in other organs or tissue such as muscle and blood had a more rapid clearance rate, which result in tumor/blood and tumor/muscle uptake ratios get much higher as time lapsed.

The most interesting part of the biodistribution data of [^{18}F] FEMPBBA is the uptake of this compound in the brain. As this compound has a high lipophilicity (log P = −0.5), it was supposed to be hard to penetrate the BBB, and the uptake in brain should be very low. However, in fact the initial [^{18}F] FEMPBBA had a relatively high initial uptake in the brain, with the activity of 1.03 ± 0.18%ID/g in the brain at 5 min.

As the time lapsed, the activity in the brain rapidly decreased to 0.19 ± 0.06%ID/g at 60 min and 0.05 ± 0.02%ID/g at 120 min. This rapid clearance rate in brain of [^{18}F] FEMPBBA made the tumor/brain uptake get a rather high ratio: 4.81 at 30 min, 7.15 at 60 min and 9.8 at 120 min.

From the biodistribution data in S180 tumor bearing mice, we can see this two compounds showed significant difference, and

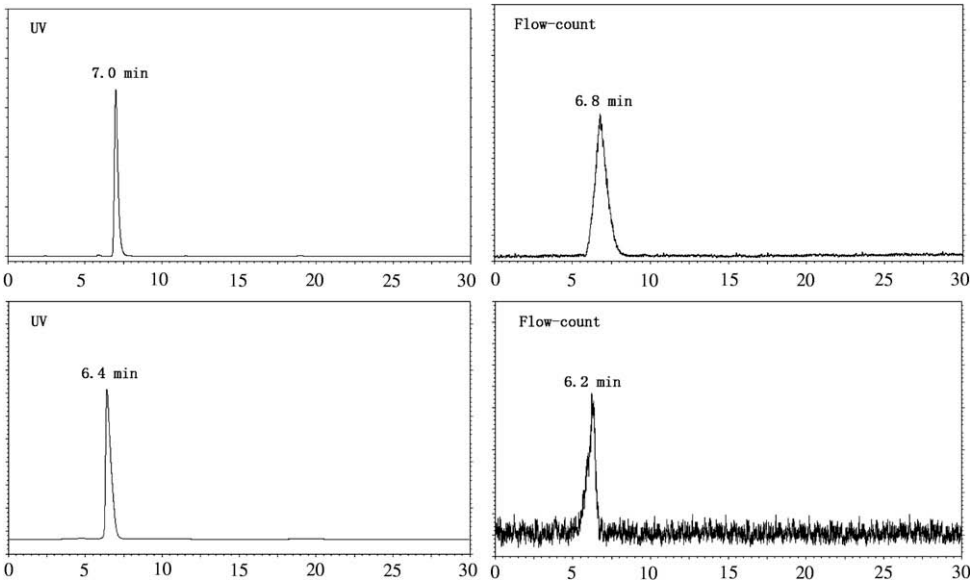

Figure 1. HPLC chromatograms of [^{18}F] FEMPBBA and [^{18}F] FNBMBBA and their corresponding ^{19}F standards.

Table 1
Biodistribution data of [^{18}F] FNBMBBA ([^{18}F] **a1**) in mice bearing S180 tumor (n = 4)

Organs	%ID/g ± SD				
	5 min	15 min	30 min	60 min	120 min
Heart	1.37 ± 0.04	0.24 ± 0.09	0.14 ± 0.02	0.06 ± 0.01	0.08 ± 0.05
Liver	8.9 ± 1.35	0.4 ± 0.07	0.66 ± 0.1	0.65 ± 0.07	0.11 ± 0.02
Pancreas	0.72 ± 0.11	0.18 ± 0.07	0.13 ± 0.03	0.07 ± 0.02	0.02 ± 0.01
Lung	1.97 ± 0.24	0.28 ± 0.13	0.14 ± 0.04	0.08 ± 0.03	0.02 ± 0.01
Kidney	8.92 ± 0.85	1.24 ± 0.17	0.43 ± 0.05	0.32 ± 0.01	0.06 ± 0.01
Stomach	0.74 ± 0.27	0.54 ± 0.21	0.44 ± 0.12	0.2 ± 0.11	0.25 ± 0.06
Muscle	0.87 ± 0.27	0.13 ± 0.07	0.1 ± 0.01	0.07 ± 0.03	0.02 ± 0.001
Blood	2.65 ± 0.63	0.37 ± 0.07	0.22 ± 0.03	0.1 ± 0.01	0.02 ± 0.01
Brain	0.13 ± 0.02	0.07 ± 0.02	0.05 ± 0.004	0.02 ± 0.01	0.01 ± 0.003
Tumor	1 ± 0.29	0.27 ± 0.13	0.19 ± 0.02	0.12 ± 0.01	0.03 ± 0.004
Tumor/blood	0.38	0.73	0.86	1.20	1.50
Tumor/muscle	1.15	2.08	1.90	1.71	1.50

the reason may not simply be the difference of Partition Coefficient of both compounds. Firstly, the uptake in tumor of two compounds shows a different trend, [^{18}F] FEMPBBA has maintained a comparably high uptake in tumor for a long time which is not seen for [^{18}F] FNBMBBA. Secondly, the [^{18}F] FEMPBBA has a much higher uptake in brain than [^{18}F] FNBMBBA while the hydrophilicities of these two compounds are both too high to penetrate the BBB (blood–brain barrier), and the initial uptake of [^{18}F] FEMPBBA is comparably high (Fig. 2). These results indicate the uptake of [^{18}F] FEMPBBA undergoes a special transport mechanism and apparently much more suitable for PET tumor imaging.

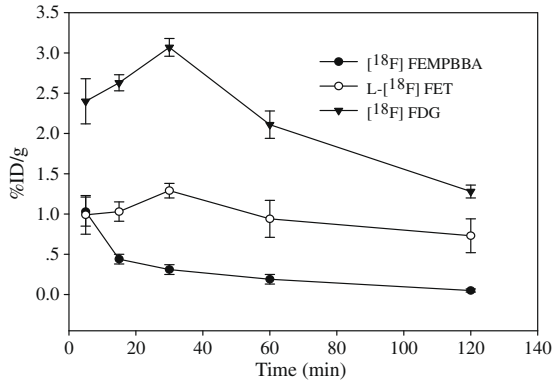

Figure 2. Time course of activity located in the brain of [^{18}F] FEMPBBA, L-[^{18}F] FET and [^{18}F] FDG. All of the data in this figure except the uptake in the brain of [^{18}F] FEMPBBA at 120 min were considered statistically significant, P <0.01, two-tailed t-test.

Parallel biodistribution experiments of [^{18}F] FDG and L-[^{18}F] FET using the same animal model was performed (Table 3 and 4) as a comparison to demonstrate the potential of [^{18}F] FNBMBBA as a PET tumor imaging agents.

From the biodistribution data of [^{18}F] FDG shown in Table 3, we can discover that the clearance rate of [^{18}F] FDG is really rapid and consequently tumor/blood uptake ratio is extremely high. On the other hand, the tumor/muscle uptake ratio of [^{18}F] FDG is also optimistic: 1.75, 2.23 and 2.20 at 30, 60 and 120 min. However, as the high uptake in the brain of [^{18}F] FDG, the tumor/brain uptake ratio is comparably low, and kept being under 1 until 60 min after injection. For L-[^{18}F] FET, the uptake in brain is much lower than [^{18}F] FDG, and it gets a quite high tumor/brain uptake ratio immediately after inject (Table 4). The tumor/brain uptake ratio of L-[^{18}F] FET gets higher as time lapse (2.54, 2.92 and 2.95 at 30, 60 and 120 min) and is much higher than that of [^{18}F] FDG.

This result is in accordance with the normal application of L-[^{18}F] FET and [^{18}F] FDG in clinical: although [^{18}F] FDG is the most widely applied PET radiopharmaceutical and have a high sensitivity for variety kinds of tumors, L-[^{18}F] FET is always used in the imaging of peripheral tumors as the contrast is by far superior to that obtained with [^{18}F] FDG because of the low uptake of L-[^{18}F] FET in normal brain tissue. As the result of biodistribution experiment was shown to be capable of reflecting the specific character of L-[^{18}F] FET and [^{18}F] FDG, we conclude the comparison of [^{18}F] FEMPBBA between them can also reflect the potential of it as a radiotracer for PET tumor imaging.

Table 2
Biodistribution data of [^{18}F] FEMPBBA ([^{18}F] **b1**) in mice bearing S180 tumor (n = 4)

Organs	%ID/g ± SD				
	5 min	15 min	30 min	60 min	120 min
Heart	4.48 ± 0.73	2.66 ± 0.48	1.76 ± 0.48	1.08 ± 0.35	0.26 ± 0.08
Liver	4.13 ± 0.25	4.02 ± 1.03	2.53 ± 0.28	1.55 ± 0.23	0.38 ± 0.12
Pancreas	2.33 ± 0.38	1 ± 0.40	1.03 ± 0.20	0.67 ± 0.31	0.2 ± 0.16
Lung	8.33 ± 1.65	5.44 ± 1.43	3.49 ± 0.35	2.35 ± 0.85	0.66 ± 0.18
Kidney	35.9 ± 1.39	13.79 ± 8.40	7.4 ± 0.65	4.2 ± 1.95	1.1 ± 0.17
Stomach	5.52 ± 0.51	4.33 ± 1.48	3.87 ± 1.32	3.23 ± 1.46	1.14 ± 0.52
Muscle	1.78 ± 0.27	1.22 ± 0.26	1.17 ± 0.05	0.62 ± 0.05	0.19 ± 0.07
Blood	3.17 ± 0.39	2.25 ± 0.77	1.36 ± 0.24	0.95 ± 0.19	0.3 ± 0.09
Brain	1.03 ± 0.18	0.44 ± 0.06	0.31 ± 0.06	0.19 ± 0.06	0.05 ± 0.02
Tumor	2.28 ± 0.27	1.41 ± 0.26	1.49 ± 0.13	1.36 ± 0.42	0.49 ± 0.09
Tumor/blood	0.72	0.63	1.09	1.43	1.63
Tumor/muscle	1.28	1.16	1.27	2.19	2.58
Tumor/brain	2.21	3.20	4.81	7.15	9.8

Table 3
Biodistribution data of [^{18}F] FDG in mice bearing S180 tumor (n = 4)

Organs	%ID/g ± SD				
	5 min	15 min	30 min	60 min	120 min
Heart	2.6 ± 0.06	2.5 ± 0.06	2.69 ± 0.14	3.24 ± 0.2	6.27 ± 0.3
Liver	1.35 ± 0.42	0.47 ± 0.17	0.23 ± 0	0.22 ± 0.04	0.2 ± 0.03
Pancreas	1.31 ± 0.4	0.95 ± 0.01	0.9 ± 0.19	0.83 ± 0.04	0.78 ± 0.18
Lung	1.52 ± 0.66	0.77 ± 0.13	0.64 ± 0.05	0.57 ± 0.06	0.52 ± 0.11
Kidney	2.16 ± 0.35	1.04 ± 0.21	0.61 ± 0.23	0.54 ± 0.15	0.25 ± 0.06
Muscle	1.56 ± 0.13	1.14 ± 0.23	1.07 ± 0.86	0.97 ± 0.66	0.78 ± 0.06
Blood	1.09 ± 0.74	0.46 ± 0.14	0.16 ± 0.01	0.11 ± 0.05	0.11 ± 0.13
Brain	2.4 ± 0.28	2.63 ± 0.1	3.07 ± 0.11	2.11 ± 0.17	1.28 ± 0.08
Tumor	1.27 ± 0.54	1.56 ± 0.23	1.86 ± 0.18	2.16 ± 0.34	1.7 ± 0.06
Tumor/blood	1.17	3.42	11.38	19.47	15.85
Tumor/muscle	0.81	1.37	1.75	2.23	2.2
Tumor/brain	0.53	0.59	0.61	1.02	1.33

Table 4
Biodistribution data of [^{18}F] FET in mice bearing S180 tumor (n = 4)

Organs	%ID/g ± SD				
	5 min	15 min	30 min	60 min	120 min
Heart	5.89 ± 1.23	3.41 ± 0.31	3.27 ± 0.37	3.14 ± 0.26	0.94 ± 0.36
Liver	7.67 ± 1.34	5.60 ± 0.30	4.23 ± 0.28	3.56 ± 0.29	1.22 ± 0.51
Pancreas	0.93 ± 0.35	0.22 ± 0.02	0.11 ± 0.07	0.03 ± 0.01	0.09 ± 0.05
Lung	16.8 ± 2.98	9.82 ± 0.45	8.57 ± 0.63	4.70 ± 0.41	1.55 ± 0.73
Kidney	6.58 ± 0.84	6.79 ± 0.23	2.38 ± 0.43	3.75 ± 0.49	1.29 ± 0.21
Muscle	2.88 ± 1.33	3.34 ± 0.41	2.69 ± 0.96	2.37 ± 0.38	2.10 ± 1.33
Blood	6.81 ± 0.95	3.30 ± 0.25	3.23 ± 0.33	2.51 ± 0.36	1.12 ± 0.37
Brain	0.99 ± 0.24	1.03 ± 0.12	1.29 ± 0.09	0.94 ± 0.23	0.73 ± 0.21
Tumor	2.08 ± 0.49	2.50 ± 0.23	3.28 ± 0.69	2.75 ± 0.36	2.15 ± 1.36
Tumor/blood	0.31	0.76	1.02	1.10	1.92
Tumor/muscle	0.72	0.75	0.62	1.23	1.02
Tumor/brain	2.10	2.43	2.54	2.92	2.95

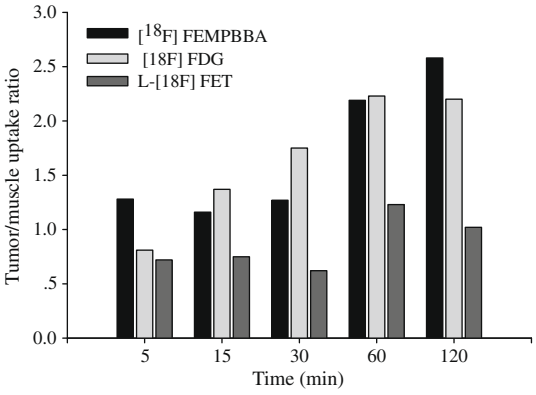

Figure 3. Comparison of tumor/muscle uptake ratios of [^{18}F] FEMPBBA with [^{18}F] FET and [^{18}F] FDG.

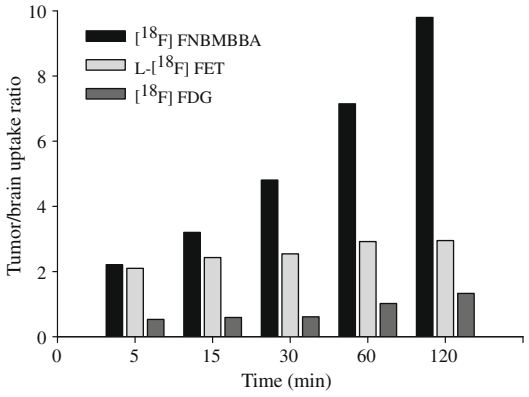

Figure 4. Comparison of tumor/brain uptake ratios of [^{18}F] FEMPBBA with [^{18}F] FET and [^{18}F] FDG.

From the comparison of [^{18}F] FEMPBBA between L-[^{18}F] FET and [^{18}F] FDG, we find [^{18}F] FEMPBBA to be competitive in some aspect.

Firstly, compared with L-[^{18}F] FET, [^{18}F] FEMPBBA has a much lower uptake in blood pool and a more rapid clearance rate from blood. That make [^{18}F] FEMPBBA get much higher tumor/blood uptake ratio than L-[^{18}F] FET at 30 min and 60 min after injection.

Secondly, [^{18}F] FEMPBBA also has a much lower uptake in muscle and a more rapid clearance rate from muscle than L-[^{18}F] FET, and get a much higher tumor/muscle uptake ratio. In contrast to [^{18}F] FDG, although the initial uptake in muscle of [^{18}F] FEMPBBA a little higher, the clearance rate of [^{18}F] FEMPBBA in muscle is more rapid than that of [^{18}F] FDG and it get a pretty much the same tumor/muscle uptake ratio as [^{18}F] FDG: 1.16, 2.19, 2.58 for [^{18}F] FEMPBBA and 1.37, 2.23, 2.2 for [^{18}F] FDG at 15 min, 60 min and 120 min. It is interesting to find that the tumor/muscle uptake ratio of [^{18}F] FEMPBBA and [^{18}F] FDG is nearly same at 60 min (2.19 for [^{18}F] FEMPBBA and 2.23 for [^{18}F] FDG), and the highest tumor/muscle uptake ratio of [^{18}F] FEMPBBA is higher than [^{18}F] FDG (Fig. 3).

The greatest advantage of [^{18}F] FEMPBBA compared with L-[^{18}F] FET and [^{18}F] FDG is the tumor/brain uptake ratio. Compared with L-[^{18}F] FET, the initial uptake of [^{18}F] FEMPBBA in brain is slightly higher, 1.03 for [^{18}F] FEMPBBA and 0.99 for L-[^{18}F] FET at 5 min. However, the clearance rate of [^{18}F] FEMPBBA from brain is really rapid, and the activity of [^{18}F] FEMPBBA get down immediately after 5 min while the uptake of L-[^{18}F] FET in brain increase at first 30 min, then decrease (Fig. 2). That make the [^{18}F] FEMPBBA has got a much higher tumor/brain uptake ratio than L-[^{18}F] FET, and certainly much higher than [^{18}F] FDG (Fig. 4).

3. Conclusion

Our attempt of developing novel ^{18}F labeled benzimidazole derivatives has turned to be encouraging. Both compounds were prepared by convenient procedures and got high radiochemical preparation yields, and the biodistribution data of two compounds in S180 tumor bearing mice has also revealed the promising prospect of benzimidazole derivatives to be applied in PET tumor imaging. The comparison of [^{18}F] FEMPBBA with [^{18}F] FDG and L-[^{18}F] FET showed it has an extremely high tumor/brain and optimistic tumor/muscle and blood uptake ratios, which indicates more investigation and experiments are needed to make further evaluation of the potential of [^{18}F] FEMPBBA and other ^{18}F labeled benzimidazole derivatives to be suitable PET tumor imaging radiotracers.

4. Methods and experimental

4.1. General

All commercial reagents and solvents were used without further purification. No-carrier-added [^{18}F] fluoride was produced by the ^{18}O(p, n)^{18}F nuclear reaction at Beijing PET Center of Xuanwu Hospital. Semipreparative HPLC column (Altech C18 column 250 × 4 mm) and analytical HPLC column (Altech C18 column 250 × 4 mm) were purchased from Altech Inc. C18 Sep-Pak Cartridge was obtained from Waters Inc.

Melting points were determined in capillary tubes using a RY-1 apparatus and are uncorrected. Nuclear magnetic resonance spectra

(^{1}H NMR and ^{13}C NMR) were performed on a Bruker spectrometer (400 M and 100 M), and chemical shifts (δ values) were reported as parts per million (ppm) downfield from tetramethylsilane (TMS). Mass spectra were recorded using a Brucker Apex IV FTM instrument at Mass Spectroscopy Center at Beijing Normal University using high-resolution electrospray ionization (ESI), or electron impact ionization (EI).

4.2. Synthesis

The preparation of compound **a2** was carried out by following the same procedure in Ref. 32, and the preparation of compound **b2** was carried out by the same procedure in Ref. 33. The preparation and the analysis data of other compounds were shown below.

4.2.1. Preparation of ethyl 4-(5-(2,4-dinitrobenzamido)-1-methyl-1*H*-benzimidazol-2-yl)butanoate (a3)

Compound **a2** (0.261 g, 1 mmol) and TEA (0.14 mL, 1 mmol) was added into CH_2Cl_2 (10 mL) and cooled to 0 °C in an ice bath. Then the solution of 2,4-dinitrobenzoyl chloride (0.23 g, 1.2 mmol) in CH_2Cl_2 (5 mL) was added dropwise. The reaction mixture was stirred in 0 °C for 0.5 h then at room temperature for 6 h. The reaction mixture was washed by $NaHCO_3$ aqueous (10 mL × 2), water (10 mL × 2), the organic layer was collected and dried over Na_2SO_4. The solvent was removed by rotary evaporation under vacuum. The crude product was recrystallized in acetic ether to give the product as yellow–green solid. (391 mg, 83% yield) mp 176–178 °C. ^{1}H NMR (400 MHz, $CDCl_3$) δ 8.73 (s, 1H, –NHCO–), 8.69 (d, J = 2.0, 1H, Ar-H), 8.35 (dd, J = 8.3, 2.1, 1H, Ar-H), 7.81 (d, J = 8.3, 1H, Ar-H), 7.59 (s, 1H, Ar-H), 7.48 (d, J = 8.6, 1H, Ar-H), 7.16 (d, J = 8.6, 1H, Ar-H), 4.04 (q, J = 7.1, 2H, –C*H*$_2$CH$_3$), 3.67 (s, 3H, N–CH$_3$), 2.82 (t, 2H, –C*H*$_2$CH$_2$CH$_2$–), 2.38 (t, J = 7.0, 2H, –CH$_2$CH$_2$C*H*$_2$–), 2.05 (m, 2H, –CH$_2$C*H*$_2$CH$_2$–), 1.18 (t, J = 7.1, 3H, –CH$_2$C*H*$_3$) ppm. ^{13}C NMR (100 MHz, $CDCl_3$) δ 173.06, 162.72, 155.69, 147.97, 146.19, 142.15, 137.93, 133.66, 131.59, 130.46, 128.23, 119.93, 116.72, 111.63, 109.23, 60.50, 33.22, 29.87, 26.59, 22.52, 14.20 ppm. MS (ESI$^+$) m/z: 456.8 (M + H$^+$). IR (KBr pellet, cm^{-1}): 3210, 1729, 1641, 1612, 1597, 1546, 1527, 1483, 1341, 1305, 1222, 1050, 1017, 906, 808, 736. Anal. Calcd for $C_{21}H_{21}N_5O_7$: C, 55.38; H, 4.65; N, 15.38. Found: C, 55.27; H, 4.73; N, 15.52.

4.2.2. Preparation of ethyl 4-(5-(2-fluoro-4-nitrobenzamido)-1-methyl-1*H*-benzimidazol-2-yl)butanoate (a4)

$Bu_4NF{\cdot}3H_2O$ (0.73 g, 2 mmol) was added into dry CH_3CN (1 mL), The solvent was evaporated under a stream of nitrogen at 78 °C in a flask, and repeated at least twice. Then the solution of compound **a3** (0.455 g, 1 mmol) in the DMF (10 mL) was added to the flask and quickly heated to 120 °C. After stirred in this temperature for 0.5 h, the reaction was cooled down and added 20 mL H_2O. The mixture was extracted with acetic ether (20 mL × 3), the organic layer was collected and evaporated by rotary evaporation under vacuum. The residue was chromatographed over a column of silica gel (A:P = 3:1) to give a yellow solid (52 yield) mp 176–178 °C. ^{1}H NMR (400 MHz, $CDCl_3$) δ 8.40 (d, J = 13.6 Hz, 1H, Ar-H), 8.34 (t, J = 8.2 Hz, 1H, Ar-H), 8.11 (dd, J = 8.6, 2.0 Hz, 1H, Ar-H), 8.02 (dd, J = 11.2, 2.0 Hz, 1H, Ar-H), 7.86 (d, J = 1.8 Hz, 1H, –NH–CO–), 7.53 (dd, J = 8.6, 1.9 Hz, 1H, Ar-H), 7.24 (d, J = 8.6 Hz, 1H, Ar-H), 4.06 (q, J = 7.1 Hz, 2H, –OC*H*$_2$CH$_3$), 3.71 (s, 3H, N–CH$_3$), 2.90 (t, J = 7.5 Hz, 2H, –C*H*$_2$CH$_2$CH$_2$–), 2.44 (t, J = 7.0 Hz, 2H, –CH$_2$CH$_2$C*H*$_2$–), 2.13 (m, J = 7.1 Hz, 2H, –CH$_2$C*H*$_2$CH$_2$–), 1.19 (t, J = 7.1 Hz, 3H, –OCH$_2$C*H*$_3$) ppm. ^{13}C NMR (100 MHz, $CDCl_3$) δ 173.12, 160.78, 158.74 (d, J_{CF} = 91.4 Hz, 1C), 155.60, 150.26 (d, J_{CF} = 10.1 Hz, 1C), 142.75, 133.69, 133.68 (d, J_{CF} = 2.5 Hz, 1C), 131.59, 127.42 (d, J_{CF} = 12.6 Hz, 1C), 119.82 (d, J_{CF} = 3.5 Hz, 1C), 116.62, 112.21 (d, J_{CF} = 30.7 Hz, 1C), 112.00, 109.13, 60.46, 33.27, 29.88, 26.71, 22.61, 14.21 ppm. ^{19}F NMR (400 MHz, $CDCl_3$) δ −109.21 ppm. MS (ESI$^+$) m/z: 429.1 (M+H$^+$). IR (KBr pellet, cm^{-1}): 3337, 1732, 1651, 1598, 1561, 1530, 1486, 1431, 1423, 1377, 1350, 1318, 1269, 1263, 1189, 813, 736. Anal. Calcd for $C_{21}H_{21}FN_4O_5$: C, 58.87; H, 4.94; N, 13.08. Found: C, 58.51; H, 5.08; N, 13.22.

4.2.3. Preparation of 4-(5-(2-fluoro-4-nitrobenzamido)-1-methyl-1*H*-benzimidazol-2-yl)butanoic acid (a1)

Compound **a4** (60 mg, 0.14 mmol) was added into CH_3CH_2OH (6 mL) and cooled to 0 °C in an ice bath, the solution of LiOH (30 mg, 0.7 mmol) in H_2O (1 mL) was then added. The reaction mixture was stirred overnight and the pH was adjusted to 2–3 with 35% HCl. The product was precipitated and filtered, the crude product was crystallized to give a light yellow solid (48 mg, 85%) mp 207–209 °C. ^{1}H NMR (400 MHz, DMSO) δ 11.22 (s, 1H, –COOH), 8.38 (d, J = 1.2 Hz, 1H, Ar-H), 8.33 (dd, J = 9.6 Hz, 2.0 Hz, 1H, Ar-H), 8.22 (dd, J = 8.4 Hz, 2.0 Hz, 1H, Ar-H), 8.02 (m, 1H, Ar-H), 7.93 (d, J = 8.9 Hz, 1H, Ar-H), 7.76 (d, J = 9.0 Hz, 1H, Ar-H), 3.96 (s, 3H, N–CH$_3$), 3.20 (t, J = 7.6 Hz, 2H, –C*H*$_2$CH$_2$CH$_2$–), 2.45 (t, J = 7.1 Hz, 2H, –CH$_2$CH$_2$C*H*$_2$–), 2.06 (m, 2H, –CH$_2$C*H*$_2$CH$_2$–) ppm. ^{13}C NMR (100 MHz, DMSO) δ 173.64, 161.41, 158.39 (d, J_{CF} = 253.0 Hz, 1C), 153.92, 149.35 (d, J_{CF} = 8.6 Hz, 1C), 136.27, 131.17 (d, J_{CF} = 3.4 Hz, 1C), 130.56, 130.40, 129.30, 119.70 (d, J_{CF} = 3.5 Hz, 1C), 117.99, 112.80, 112.10 (d, J_{CF} = 27.3 Hz, 1C), 104.54, 32.53, 30.99, 24.42, 21.30 ppm. ^{19}F NMR (400 MHz, $CDCl_3$) δ −111.08 ppm. MS (ESI$^+$) m/z: 401.5 (M+H$^+$). IR (KBr pellet, cm^{-1}): 3432, 3043, 1724, 1682, 1624, 1562, 1529, 1500, 1446, 1419, 1352, 1287, 1191, 816, 739. Anal. Calcd for $C_{19}H_{17}FN_4O_5$: C, 57.00; H, 4.28; N, 13.99. found: C, 56.76; H, 4.53; N, 13.87.

4.2.4. Preparation of methyl 7-methyl-2-propyl-3-(2-(tosyloxy)ethyl)-3*H*-benzimidazole-5-carboxylate (b3)

To a 20 mL dried THF, NaH (0.18 g, 7.5 mmol) was dissolved and the solution was stirred in an ice bath. Then compound **b2** (0.58 g, 2.5 mmol) was added portionwise. After stirred in room temperature for another 1 h, ethyleneglycol-1,2-ditosylate (5 mmol) was added and the reaction mixture was stirred in 40–50 °C overnight. The solvent was removed and the residue was chromatographed over a column of silica gel (A:P = 3:1) to give a white solid. (0.45 g, 42% yield) mp 167–168 °C. ^{1}H NMR (400 MHz, $CDCl_3$) δ 7.65 (s, 1H, Ar-H), 7.54 (s, 1H, Ar-H), 7.34 (d, J = 8.3 Hz, 2H, Ar-H), 6.94 (d, J = 8.1 Hz, 2H, Ar-H), 4.33 (t, J = 5.1 Hz, 2H, –CH$_2$CH$_2$–OTs), 4.26 (t, J = 5.1, 2H, –CH$_2$CH$_2$–OTs), 3.86 (s, 3H, –OCH$_3$), 2.79 (t, J = 8.0 Hz, 2H, –CH$_2$CH$_2$CH$_3$), 2.58 (s, 3H, Ar-CH$_3$), 2.23 (s, 3H, Ar-CH$_3$), 1.79 (m, 2H, –CH$_2$CH$_2$CH$_3$), 0.99 (t, J = 7.3 Hz, 3H, –CH$_2$CH$_2$CH$_3$) ppm. ^{13}C NMR (100 MHz, $CDCl_3$) δ 167.5, 157.5, 145.6, 145.0, 133.4, 131.4, 129.6, 129.0, 127.4, 123.9, 123.8, 108.4, 66.4, 52.0, 42.6, 29.4, 21.7, 21.5, 16.7, 14.0 ppm. MS (ESI$^+$) m/z: 431.1 (M+H$^+$). IR (KBr pellet, cm^{-1}): 1702, 1436, 1359, 1340, 1279, 1249, 1205, 1193, 1180, 1009, 899, 769, 664, 554. Anal. Calcd for $C_{22}H_{26}N_2O_5S$: C, 61.38; H, 6.09; N, 6.51. Found: C, 61.53; H, 6.34; N, 6.73.

4.2.5. Preparation of methyl 3-(2-fluoroethyl)-7-methyl-2-propyl-3*H*-benzimidazole-5-carboxylate (b4)

To a 20 mL dried THF, NaH (0.29 g, 12 mmol) was dissolved and the solution was stirred in an ice bath. Then compound **b3** (0.93 g, 4 mmol) was added portionwise. After being stirred in room temperature for another 1 h, 1-bromo-2-fluoroethane (1.4 mL, 13 mmol) was added dropwise and the reaction mixture was stirred in 40–50 °C overnight. The solvent was removed and the residue was chromatographed over a column of silica gel (A:P = 2:1) to give a white solid. (0.48 g, 83% yield). mp 103–105 °C. ^{1}H NMR (400 MHz, $CDCl_3$) δ 7.78 (s, 1H, Ar-H), 7.72 (s, 1H, Ar-H), 4.68 (dt, J = 46.8, 4.7 Hz, 2H, –CH$_2$C*H*$_2$F), 4.39 (dt, J = 25.6 Hz, 4.6 Hz, 2H,

–CH_2CH_2F), 3.87 (s, 3H, –OCH_3), 2.61 (s, 3H, –CH_3), 2.60 (s, 3H, –CH_3) ppm. ^{13}C NMR (100 MHz, $CDCl_3$) δ 167.74, 154.29, 145.53, 134.12, 128.98, 124.07, 123.92, 108.61, 81.40 (d, J_{CF} = 173.4 Hz, 1C), 52.14, 44.40 (d, J_{CF} = 21.4 Hz, 1C), 16.67, 14.17 (d, J_{CF} = 2.5 Hz, 1C) ppm. ^{19}F NMR (400 MHz, $CDCl_3$) δ −221.32 ppm. MS (ESI^+) *m*/*z*: 251.0 ($M+H^+$). IR (KBr pellet, cm^{-1}): 1712, 1518, 1435, 1408, 1346, 1292, 1274, 1232, 1215, 1203, 1034, 764. Anal. Calcd for $C_{13}H_{15}FN_2O_2$: C, 62.39; H, 6.04; N, 11.19. Found: C, 62.43; H, 6.11; N, 11.08.

4.2.6. Preparation of 3-(2-fluoroethyl)-7-methyl-2-propyl-3*H*-benzimidazole-5-carboxylic acid (b1)

Compound **b4** (0.22 g, 0.79 mmol) was added into CH_3OH (7 mL) and cooled to 0 °C in an ice bath, the aqueous solution of NaOH (10%, 3 mL) was then added. The reaction mixture was stirred overnight and the pH was adjusted to 2–3 with 35% HCl. The product was precipitated and filtered, and the crude product was crystallized to give a light white solid. (0.19 g, 90% yield) mp 237–239 °C. ^1H NMR (400 MHz, DMSO) δ 7.99 (s, 1H, Ar-H), 7.62 (s, 1H, Ar-H), 4.78 (s, 1H, –CH_2CH_2F), 4.66 (s, 2H, –CH_2CH_2F), 4.59 (s, 1H, –CH_2CH_2F), 2.87 (t, *J* = 7.6 Hz, 2H, –$CH_2CH_2CH_3$), 2.54 (s, 3H, Ar-CH_3), 1.83 (m, 2H, –$CH_2CH_2CH_3$), 1.01 (t, *J* = 7.3 Hz, 3H, –$CH_2CH_2CH_3$) ppm.^{13}C NMR (100 MHz, DMSO) δ 167.96, 157.41, 144.95, 134.31, 127.44, 123.89, 122.87, 109.79, 82.56 (d, J_{CF} = 167.8 Hz, 1C), 43.52 (d, J_{CF} = 19.6 Hz, 1C), 28.41, 20.41, 16.26, 13.81 ppm. ^{19}F NMR (400 MHz, $CDCl_3$) δ −220.70 ppm. MS (ESI^+) *m*/*z*: 265.1 ($M+H^+$). IR (KBr pellet, cm^{-1}): 3448, 2960, 2929, 1687, 1613, 1595, 1459, 1413, 1348, 1248, 1227, 1215, 1189, 1098, 1041, 1020, 897, 777, 707. Anal. Calcd for $C_{14}H_{17}FN_2O_2$: C, 63.62; H, 6.48; N, 10.60. Found: C, 63.45; H, 6.63; N, 10.45.

4.2.7. Radiochemistry

$[^{18}F]$ fluoride was generated from $H_2[^{18}O]$-enriched water via proton bombardment. The $[^{18}F]$ fluoride was absorbed on an anion exchange cartridge, and eluted with an aqueous mixture of 10 mg $K_{2.2.2}$ and 3 mg K_2CO_3 in 0.5 mL CH_3CN and 1 mL H_2O to get $[^{18}F]$ $K_{2.2.2}$/KF complex. The solvent was evaporated under a stream of nitrogen at 90 °C. Azeotropic drying was repeated more than twice with 1 mL portions of CH_3CN.

However, as the leaving group of two compounds is different, the condition of the substitution reaction is also different. After the azeotropic drying was completed, the solution of approximately 4–5 mg **a4** in 2 mL dry DMF for $[^{18}F]$ FNBMBBA (2 mL dry CH_3CN and 4–5 mg **b3** for $[^{18}F]$ FEMPBBA) was added to the vial containing $[^{18}F]$ $K_{2.2.2}$/KF complex. The solution was heated to 115 °C (90 °C for $[^{18}F]$ FEMPBBA) for 20 min.

Compound $[^{18}F]$ FEMPBBA was purified just by Sep-Pak Silica Plus cartridge and compound $[^{18}F]$ FNBMBBA was purified by HPLC (Altech C18 column 250 × 4 mm, CH_3CN/H_2O = 70:30 [vol/vol], 3 mL/min) The elution was collected after purification and solvent was removed under a stream of nitrogen at 110 °C. Then hydrolysis was performed using LiOH (10 mg) in MeOH (2 mL) at room temperature for 10 min and pH was adjusted to 7 with 1 N HCl immediately to afford $[^{18}F]$ FNBMBBA and $[^{18}F]$ FEMPBBA. The solvent was then evaporated and the products were solved in saline prepared for further use.

4.3. Pharmacological studies

4.3.1. Stability in plasma

The determination of the stability in plasma of both compounds was carried out by HPLC analysis.

After incubation of $[^{18}F]$ FNBMBBA or $[^{18}F]$ FEMPBBA (100–150 μCi, 50 μL) in 0.5 mL mice plasma for 3 h, the plasma was added in 1 mL CH_3CN then centrifuged for 5 min at 13,200 rpm. The supernatants part was passed through a C18 Sep-Pak Cartridge, and the cartridge was washed with water (2 mL × 2), then eluted with 2 mL of CH_3CN containing 0.1% TFA. The result of HPLC analysis indicates the two compounds were both stable in plasma.

4.3.2. Measurement of partition coefficient

The partition coefficient of $[^{18}F]$ FNBMBBA and $[^{18}F]$ FEMPBBA was measured using 2.5 mL *n*-octanol as the organic phase and 2.5 mL 0.01 M PBS (pH 7.4) as the water phase. 0.01 mL radioactive sample of $[^{18}F]$ FNBMBBA or $[^{18}F]$ FEMPBBA was added. After being vigorously mixed for 5 min at room temperature, the radioactivity of 0.01 mL of each phase was measured after centrifugation.

4.3.3. Biodistribution in S180 bearing mice

The biodistribution experiments of both compounds were carried out with the same procedure.

Female Kunming mice with S180 were prepared for biodistribution studies. The S180 tumor model was generated by subcutaneous injection of 5×10^6 tumor cells into the right front flank of Female Kunming mice without anesthesia. The experiment was performed after the tumor cells were inoculated for 7–14 days, at which time the mice weighed between 18–22 g. Each animal was injected with saline solvent of $[^{18}F]$ FNBMBBA or $[^{18}F]$ FEMPBBA (10–20 μCi, 100 μL) via the tail vein, then sacrificed at 5, 15, 30, 60 and 120 min post injection. The interested organs and tissue samples were excised immediately, blotted to remove adhering blood, weighed, and the radioactivity was measured using a gamma counter. The uptake of radiotracer in organs or tissue was expressed in counts per second (cps) with decay correction normalized as mean ± SD (%ID/g, n = 4), and the statistics were performed by two-tailed *t*-test.

Acknowledgments

We acknowledged with thanks for financial supports from the National Science foundation of China (No. 20371009 and 20671014) and Beijing Municipal Commission of Education. We also would like to thank the cyclotron operator team of the PET Centre of Xuan Wu hospital, for providing $[^{18}F]$ fluoride activity and technical assistance.

References and notes

1. Ansari, K. F.; Lal, C. *Eur. J. Med. Chem.* **2009**, *44*, 2294.
2. Goker, H.; Ozden, S.; Yildiz, S.; Boykin, D. W. *Eur. J. Med. Chem.* **2005**, *40*, 1062.
3. Sondhi, S. M.; Singh, N.; Kumar, A.; Lozach, O.; Meijer, L. *Bioorg. Med. Chem.* **2006**, *14*, 3758.
4. Mor, M.; Bordi, F.; Silva, C.; Rivara, S.; Zuliani, V.; Vacondio, F.; Rivara, M.; Barocelli, E.; Bertoni, S.; Ballabeni, V.; Magnanini, F.; Impicciatore, M.; Plazzi, P. V. *Bioorg. Med. Chem.* **2004**, *12*, 663.
5. Rivara, M.; Zuliani, V.; Cocconcelli, G.; Morini, G.; Comini, M.; Rivara, S.; Mor, M.; Bordi, F.; Barocelli, E.; Ballabeni, V.; Bertoni, S.; Plazzi, P. V. *Bioorg. Med. Chem.* **2006**, *14*, 1413.
6. Demirayak, S.; Abu Mohsen, U.; Karaburun, A. C. *Eur. J. Med. Chem.* **2002**, *37*, 255.
7. Yamori, T.; Matsunaga, A.; Sato, S.; Yamazaki, K.; Komi, A.; Ishizu, K.; Mita, I.; Edatsugi, H.; Matsuba, Y.; Takezawa, K.; Nakanishi, O.; Kohno, H.; Nakajima, Y.; Komatsu, H.; Andoh, T.; Tsuruo, T. *Cancer Res.* **1999**, *59*, 4042.
8. Nawrocka, W.; Sztuba, B.; Kowalska, M. W.; Liszkiewicz, H.; Wietrzyk, J.; Nasulewicz, A.; Pelczynska, M.; Opolski, A. *Farmaco (Lausanne)* **2004**, *59*, 83.
9. Agic, D.; Hranjec, M.; Jajcanin, N.; Starcevic, K.; Karminski-Zamola, G.; Abramic, M. *Bioorg. Chem.* **2007**, *35*, 153.
10. Ismail, M. A.; Brun, R.; Wenzler, T.; Tanious, F. A.; Wilson, W. D.; Boykin, D. W. *Bioorg. Med. Chem.* **2004**, *12*, 5405.
11. Starcevic, K.; Krajl, M.; Ester, K.; Sabol, I.; Grce, M.; Pavelic, K.; Karminski-Zamola, G. *Bioorg. Med. Chem.* **2007**, *15*, 4419.
12. Plosker, G. L.; Carter, N. J. *Drugs* **2008**, *68*, 2645.
13. Bremer, K. *J. Cancer Res. Clin. Oncol.* **2002**, *128*, 603.
14. Bresch, S.; Fassbender, V.; Wei, L.; Ticchioni, M.; Manonne, L.; Mounier, N. *Oncologie* **2009**, *11*, 473.
15. Friedberg, J. W. *Leuk. Lymphoma* **2009**, *50*, 1399.
16. Eichbaum, M. H. R.; Schuetz, F.; Khbeis, T.; Lauschner, I.; Foerster, F.; Sohn, C.; Schneeweiss, A. *Anti-Cancer Drug* **2007**, *18*, 963.
17. Konstantinov, S. M.; Kostovski, A.; Topashka-Ancheva, M.; Genova, M.; Berger, M. R. *J. Cancer Res. Clin. Oncol.* **2002**, *128*, 271.

18. Koster, W.; Heider, A.; Niederle, N.; Wilke, H.; Stamatis, G.; Fischer, J. R.; Koch, J. A.; Stahl, M. *J. Thoracic Oncol.* **2007**, *2*, 312.
19. Schmittel, A.; Knodler, M.; Hortig, P.; Schulze, K.; Thiel, E.; Keilholz, U. *Lung Cancer* **2007**, *55*, 109.
20. Kalaycio, M. *Cancer* **2009**, *115*, 473.
21. Leoni, L. M.; Bailey, B.; Reifert, J.; Bendall, H. H.; Zeller, R. W.; Corbeil, J.; Elliott, G.; Niemeyer, C. C. *Clin. Cancer Res.* **2008**, *14*, 309.
22. Phelps, M. E. *Proc. Natl. Acad. Sci. U.S.A.* **2000**, *97*, 9226.
23. Miller, P. W.; Long, N. J.; Vilar, R.; Gee, A. D. *Angew. Chem., Int. Ed.* **2008**, *47*, 8998.
24. Hoh, C. K. *Nucl. Med. Biol.* **2007**, *34*, 737.
25. Varagnolo, L.; Stokkel, M. P. M.; Mazzi, U.; Pauwels, E. K. J. *Nucl. Med. Biol.* **2000**, *27*, 103.
26. Balogova, S.; Perie, S.; Kerrou, K.; Grahek, D.; Montravers, F.; Angelard, B.; Susini, B.; El Chater, P.; St Guily, J. L.; Talbot, J. *Eur. J. Nucl. Med. Mol. I* **2007**, *34*, S131.
27. Pauleit, D.; Zimmermann, A.; Stoffels, G.; Bauer, D.; Risse, J.; Fluss, M. O.; Hamacher, K.; Coenen, H. H.; Langen, K. J. *J. Nucl. Med.* **2006**, *47*, 256.
28. Reske, S. N.; Deisenhofer, S. *Eur. J. Nucl. Med. Mol. I* **2006**, *33*, S38.
29. Wester, H. J.; Herz, M.; Weber, W.; Heiss, P.; Senekowitsch-Schmidtke, R.; Schwaiger, M.; Stocklin, G. *J. Nucl. Med.* **1999**, *40*, 205.
30. Wang, H. E.; Wu, S. Y.; Chang, C. W.; Liu, R. S.; Hwang, L. C.; Lee, T. W.; Chen, J. C.; Hwang, J. J. *Nucl. Med. Biol.* **2005**, *32*, 367.
31. Chen, W.; Cloughesy, T.; Kamdar, N.; Satyamurthy, N.; Bergsneider, M.; Liau, L.; Mischel, P.; Czernin, J.; Phelps, M. E.; Silverman, D. H. S. *J. Nucl. Med.* **2005**, *46*, 945.
32. Ozegowski, W.; Krebs, D. *J. Prakt. Chem. IV* **1963**, *20*, 178.
33. Ries, U. J.; Mihm, G.; Narr, B.; Hasselbach, K. M.; Wittneben, H.; Entzeroth, M.; Vanmeel, J. C. A.; Wienen, W.; Hauel, N. H. *J. Med. Chem.* **1993**, *36*, 4040.